Synthesis and characterization of single crystals of the superconductors $Hg_{0.8}Bi_{0.2}Ba_2Ca_{n-1}Cu_nO_{2n+2+\delta}$ ($n=2,3$)

D. Pelloquin, V. Hardy, and A. Maignan*
Laboratoire CRISMAT, ISMRA et Université de Caen, URA 1318 associée au CNRS, Boulevard du Maréchal Juin, 14050 Caen Cedex, France
(Received 24 June 1996)

Single crystals of the 1212 ($n=2$) and 1223 ($n=3$) mercury based cuprates have been grown using Bi_2O_3 as a flux during the growth. The bismuth cations act as stabilizers of the structures which do not require the use of a dry box or high pressure. Electron microscopy and coupled energy dispersive spectroscopy analyses evidence the regularity of the 1212 and 1223 structures with a mercury layer of composition close to $Hg_{0.8}Bi_{0.2}$. Moreover the structural refinements based on x-ray-diffraction data of these crystals, show at the level of the $[(Hg,Bi)O_\delta]$ layer a splitting of the oxygen site around the position $(\frac{1}{2}\frac{1}{2}0)$. These as-grown superconducting crystals exhibit critical temperatures of 121 and 130 K for 1212 and 1223, respectively. The irreversibility lines (IL) and fishtail lines (FL) of these crystals are compared to those of (Hg,Bi)-1201 crystals and grain aligned Hg-1223 ceramics. These data show that the $Hg_{0.8}Bi_{0.2}$-1223 IL and FL lie above that of $Hg_{0.8}Bi_{0.2}$-1212. This suggests that the anisotropy of 1223 is smaller than that of 1212. The similarity of the FL's location of isostructural Tl-1223 and $Hg_{0.8}Bi_{0.2}$-1223 illustrates the role of the structure on the superconducting properties. [S0163-1829(96)08246-X]

INTRODUCTION

The mercury-based copper oxides form a large family of superconductors with the generic formulation $HgBa_2Ca_{n-1}Cu_nO_{2n+2+\delta}$ with $1 \leqslant n \leqslant 5$.[1,2] The two members $HgBa_2CaCu_2O_{6+\delta}$ ($n=2$ abbreviated 1212) and $HgBa_2Ca_2Cu_3O_{8+\delta}$ ($n=3$ abbreviated 1223), that exhibit high T_c's of 125 and 133 K respectively,[2] are potential candidates for future applications and from a more fundamental point of view their discovery should give new data for the understanding of the copper oxides superconductivity. However, owing to the two-dimensional (2D) character of the superconducting cuprates, their superconducting properties are anisotropic and oriented materials are required in order to study their properties. Unfortunately, three years after their discover, only two phases have been isolated in single crystal form $HgBa_2Ca_2Cu_3O_{8+\delta}$ (1223) (Ref. 3) and $HgBa_2Ca_3Cu_4O_{10+\delta}$ (1234) (Ref. 4) which correspond to the $n=3$ and $n=4$ members of the mercury series respectively. No data concerning the physical properties of single-crystals for the two first members $HgBa_2CuO_{4+\delta}$ (1201) and $HgBa_2CaCu_2O_{6+\delta}$ (1212) have been published to date. In fact, as described in Ref. 5, both $n=1$ and $n=2$ members are needed to complete the existing superconducting data—electronic anisotropy, irreversibility lines, superconducting parameters such as λ_{ab}, H_{c_2}—in order to understand the role of the copper layer number n on the physical properties.

The synthesis difficulties of the mercury-based cuprates are linked to the decomposition of HgO and to the great sensitivity of the precursors to impurities. Two different ways have been taken to overcome this problem: low-temperature syntheses to grow Hg-1223 crystals[3] and a high-pressure technique to grow Hg-1234 crystals.[4] A third route was also investigated in order to stabilize these phases in ceramic form which involved introducing a foreign cation on the mercury site.[6] This stabilizer must exhibit a higher valence than Hg^{II} to allow the oxygen vacancies in the $[HgO_\delta]$ layer to be partially filled. Among ten cations that have been shown to be efficient as stabilizers,[6] bismuth was very attractive since this cation may play the role of flux during crystal growths. This was recently demonstrated by crystal growth of the $n=1$ member $Hg_{0.8}Bi_{0.2}CuO_{4+\delta}$ (Ref. 7) whose structure and magnetic properties were investigated. In the present paper we report on the synthesis, structural and magnetic characterizations of the $Hg_{0.8}Bi_{0.2}Ba_2CaCu_2O_{6+\delta}$ and $Hg_{0.8}Bi_{0.2}Ba_2Ca_2Cu_3O_{8+\delta}$ superconducting single crystals, corresponding to the $n=2$ and $n=3$ members of the series.

CRYSTAL GROWTH AND STRUCTURAL CHARACTERIZATIONS

The (Hg,Bi)-1212 and (Hg,Bi)-1223 single crystals investigated here were synthesized from precursor pellets without

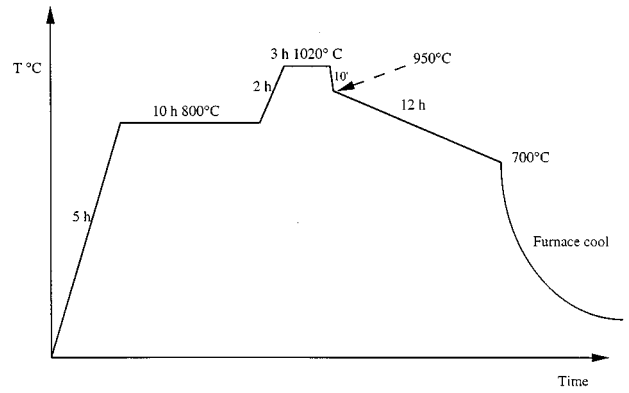

FIG. 1. Thermal cycle used for $Hg_{0.8}Bi_{0.2}Ba_2CaCu_2O_{6+\delta}$ (1212) and $Hg_{0.8}Bi_{0.2}Ba_2Ca_2Cu_3O_{8+\delta}$ (1223) single-crystal growth.

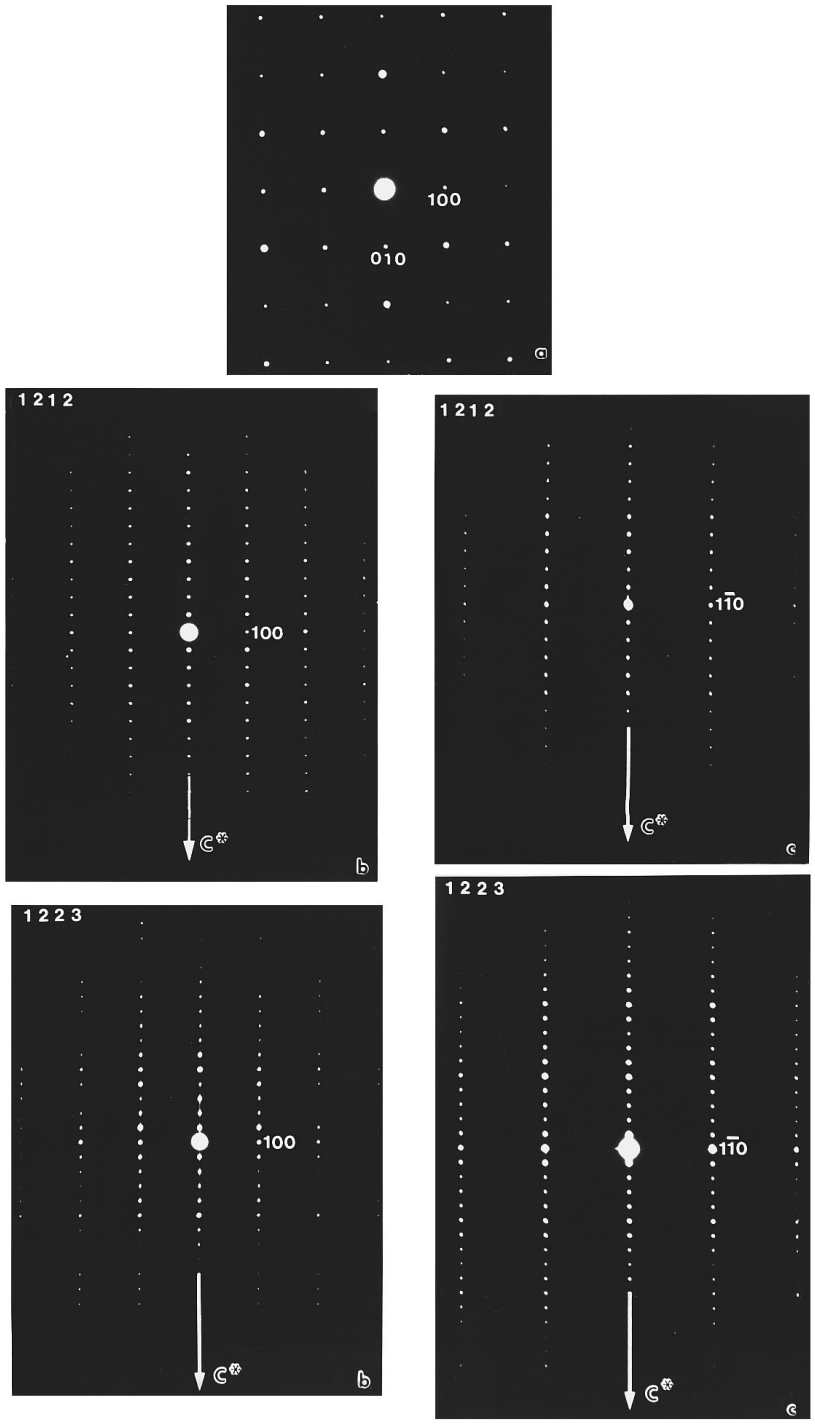

FIG. 2. ED patterns of $Hg_{0.8}Bi_{0.2}Ba_2CaCu_2O_{6+\delta}$ (1212), $Hg_{0.8}Bi_{0.2}Ba_2Ca_2Cu_3O_{8+\delta}$ (1223) single-crystal fragment (a): [001]; (b): [100]; (c): [110].

using dry box or high-pressure techniques. Two precursor pellets, with nominal compositions $Ba_2CaCu_2O_x$ (preparation A) and $Ba_2Ca_2Cu_3O_x$ (preparation B) respectively, were prepared from a well-ground stoichiometric mixture of $Ba(NO_3)_2$, CaO, and CuO by reacting at 920 °C under an oxygen flow for 12 h. A stoichiometric amount of yellow HgO and Bi_2O_3, according to the ratio 0.8:0.1, was then added to each precursor pellet and the mixtures were thoroughly ground. Each powder was placed in an alumina crucible (height 50 mm, inner diameter 5 mm) sealed in an evacuated silica tube (height 90 mm, inner diameter 9 mm) and then introduced in a vertical furnace to undergo the thermal cycle described in Fig. 1. Note that the position of the tubes with regard to the middle of the furnace (hot part) is fundamental to controlling the crystal growth of each structural type. Therefore, a little shift of about 10 mm with regard to this position modifies the nature of the as-grown phase. With this method, a multiphasic sample, with a few little droplets of mercury, was obtained for each preparation: a brick red matrix ceramic is observed in the upper part of the crucible (cold part), while in the lower part (near the hot part) clusters of black and shiny platelike crystals of about

TABLE I. Crystallographic data.

Crystal data	
Space group	$P4/mmm$ ($n°$ 123)
Cell dimensions	$a=3.8565$ (3) Å
	$c=12.711$ (1) Å
Volume	189.05 (3) Å^3
Z	1
ρ_{calc}	6.501 g/cm^3
Intensity measurements	
λ(MoKα)	0.71073 Å
Scan mode	ω-θ
Scan width	$1.1+0.35\tan\theta$
Slit aperture	$1.1+\tan\theta$
Max θ	45°
Measured reflections	544
Standard reflections	3
Reflections width $I>3\sigma$	409
μ (cm^{-1})	372.7
Structure refinement	
Parameters refined	20
Absorption correction	based on the morphology
Program used	XTAL
Computer determination	PC
Agreement factors	difference Fourier synthesis

$300\times300\times10$ μm^3 were observed.

Several crystals were extracted in each preparation for a preliminary x-ray-diffraction study. The Weissenberg patterns allowed the quality of crystals to be checked and the 1212 and 1223 structures to be identified in the preparations A and B respectively. For these as-synthesized single crystals, magnetization measurements performed with a superconducting quantum interference device (SQUID) magnetometer with $\mu_0 H=10^{-3}$ T, showed two distinct superconducting behaviors, below about 120 K (A) and 130 K (B) respectively. Fragments of these crystals were then studied by electron diffraction (ED) with a JEOL 200 Cx microscope equipped with an eucentric goniometer (±60°). The [001], [100], and [110] ED patterns for both single-crystal types (Fig. 2) evidenced a tetragonal symmetry with $a=a_p\approx3.8$ Å and $c\approx12.7$ Å (type 1212) and $c\approx15.8$ Å (type 1223). No streaks or additional reflections were observed. The EDS analysis performed with a Kevex analyser showed that the cationic composition is consistent from one crystal to the other for the same sample and very close to the nominal stoichiometry. In particular, both single-crystal types exhibit the same ratio Hg/Bi, 0.75:0.25, similarly to the ratio observed in the (Hg,Bi)-1201 single crystals previously studied[7] which corresponds to the first member ($n=1$) of the $(Hg_{0.8}Bi_{0.2})Ba_2Ca_{n-1}Cu_nO_{2n+2+\delta}$ series. For the clarity of the text, in the following, the Hg and Bi compositions will be corrected to 0.8 and 0.2 respectively.

A detailed structural study has been performed in order to confirm both structural models. This work was carried out simultaneously by high-resolution electron microscopy (HREM) and by x-ray diffraction. The single crystal x-ray data were recorded by means of a four circles CAD 4 Enraf Nonius diffractometer at 20 °C, using a graphite monochromatized MoKα radiation (λ=0.710 74 Å), while HREM images were recorded from a TOPCON 02B electron microscope operating at 200 kV and having a resolution of 1.8 Å.

The structures of both single-crystal types, $Hg_{0.8}Bi_{0.2}$-1212 and $Hg_{0.8}Bi_{0.2}$-1223, were refined in the space group $P4/mmm$ ($n°$ 123). The starting positional parameters were those obtained from powder-neutron-diffraction data.[2] The same procedure in both cases was applied for the structure determination. The refinements of both structures fit perfectly well with the data (cell parameters, cationic positions) reported for the pure mercury single crystals.[8] Only the results of the $Hg_{0.8}Bi_{0.2}$-1212 single crystal have therefore been illustrated in Tables I–III. The most important difference with regard to the bismuth free Hg-12($n-1$)n single crystals is observed at the level of the mixed layer [$(Hg_{0.8}Bi_{0.2})O\delta$]. As mentioned previously, in the study of $(Hg_{0.8}Bi_{0.2})$-1201 single crystals,[7] the oxygen site is neither in position ($\frac{1}{2}00$) nor in position ($\frac{1}{2}\frac{1}{2}0$) but it is split around this later position. This structural phenomenon is clearly shown in the Fourier map obtained before any refinements [Fig. 3(a)]. Locating this oxygen and refining its position accurately is not easy by x-ray diffraction but the analysis of the difference Fourier map performed during the last refinements [Fig. 3(b)] showed several residual electron density peaks around the theoretical position ($\frac{1}{2}\frac{1}{2}0$) especially one peak of about $4e^-/$Å^3 at ($\frac{1}{2}$ 0.31 0). Note that the same phenomenon is also observed in single crystals corresponding to the member $n=3$ of the series.

Finally, HREM images were recorded along the [100] di-

TABLE II. Final positional parameters ($R_i=0.052$) and their estimated standard deviations (ESD).

Atom	Site	x	y	z	B_{eq} (Å^2)	τ
Hg/Bi	1a	0.022(5)	0	0	1.36(3)	0.75/0.25
Ba	2h	1/2	1/2	0.2195(1)	0.87(3)	1
Ca	1d	1/2	1/2	1/2	0.87(3)	1
Cu	1b	0	0	0.3757(2)	0.47(7)	1
O(1)	2e	1/2	0	0.377(1)	0.9(4)	1
O(2)	2g	0	0	0.158(2)	2.04(4)	1
O(3)	4j	0.33(4)	0.33(4)	0	1.0[a]	0.08(5)
O′(3)	4j	0.30(7)	1/2	0	1.0[a]	0.06(5)

[a]Values fixed according to intermediate refinements.

TABLE III. General displacement parameter expressions U_{ij}.

Atom	U_{11}	U_{22}	U_{33}	U_{12}	U_{13}	U_{23}
Hg/Bi	0.005(4)	U_{11}	0.0079(5)	−0.005(6)	0	0
Ba	0.064(3)	U_{11}	0.0112(6)	0	0	0
Ca	0.006(1)	U_{11}	0.006(2)	0	0	0
Cu	0.0012(6)	U_{11}	0.0067(9)	0	0	0
O(1)	0.009(4)	-	-	-	-	-
O(2)	0.02(4)	-	-	-	-	-
O(3)	0.01	-	-	-	-	-
O′(3)	0.01	-	-	-	-	-

rection (Fig. 4 and 5) to confirm the stacking layer mode of the 1212 and 1223 structures. In the [100] image of the $(Hg_{0.8}Bi_{0.2})$-1223 microcrystal (Fig. 4), the bright dots are correlated to the zones of high electron density. We clearly observe a group of three rows of staggered bright dots correlated to the BaO-$(Hg_{0.8}Bi_{0.2})$-BaO layers. Three other rows of bright dots, spaced 3.2 Å apart, are correlated to the copper layers (arrow heads) and are separated by two rows of small grey dots associated with the calcium layers (small arrows). In the same way, fragments of $(Hg_{0.8}Bi_{0.2})$-1212 single crystals have been studied. In the image displayed in Fig. 5(a), recorded with a defocus value close to −250 Å, cations appear as dark dots while in the second image [Fig. 5(b)] recorded for a focus value close to −500 Å, cations appear as bright dots. As described above, we observe groups of three rows characteristic of the BaO-$(Hg_{0.8}Bi_{0.2})$-BaO layers (white arrows) which are separated by only two (instead of three) rows of grey dots (arrow heads on Fig. 5); these rows are correlated to the copper layers.

Therefore, these two types of sequence can be easily interpreted as the stacking modes of the 1223 and 1212 structures respectively. Note that the layer sequences are highly regular. Moreover, the even contrast observed at the level of the intermediate Hg/Bi layer, whatever the viewing direction, shows there is no short-range ordering between Hg/Bi and oxygen/vacancies.

SUPERCONDUCTING PROPERTIES

For both $Hg_{0.8}Bi_{0.2}$-1212 and $Hg_{0.8}Bi_{0.2}$-1223 batches several crystals with typical dimensions $300\times300\times100$ μm^3 were extracted and tested in order to check their T_c homogeneities. All the superconducting properties were investigated by dc magnetization (M) measurements ($0\leqslant\mu_0 H\leqslant5$ T) with a SQUID magnetometer. The measurements were limited to the $H\|c$ geometry which corresponds to supercurrents flowing in the ab plane. The sample holder used in the magnetometer was rigid (20 cm) and guided by two O rings at its ends (at better than 1 mm) ensuring a maximum deviation of 0.3° between the magnetic field and the sample holder axis. For each run of measurements, the crystal was glued with silicon grease in the geometry $H\|c$ and the quality of the alignment (larger external faces perpendicular to the holder axis) was controlled to be less than 1°. The misalignment between the crystal c axis and the magnetic field was found to be smaller than 2.5°. This small misalignment ensures the validity of the magnetization data.

In order to characterize the superconducting transitions, $M(T)$ curves were registered under 10^{-3} T after zero-field cooling. The T_c (onset) of $Hg_{0.8}Bi_{0.2}$-1223 as-grown crystals was found to be very reproducible from one crystal to the other [T_c (onset)=130 K] and the broadness of the transition was found to be close to ΔT_c (10%–90%)=4 K. One typical curve is given in Fig. 6. For $Hg_{0.8}Bi_{0.2}$-1212, ten crystals were tested exhibiting a constant T_c (onset)=121 K with a transition broadness of ΔT (10%–90%)=10 K, i.e., 6 K larger than that of the 1223 crystals. One curve is also shown in Fig. 6 and one can notice that internal susceptibilities χ_i calculated from the relation $\chi_i=\chi_{ext}/(1-\eta\chi_{ext})$, where χ_{ext} and η correspond to the external susceptibility and to the demagnetization factor respectively, are close to −1 on the low-T side attesting of the good shielding of the crystals. For comparison the $\chi_i(T)$ curve of a $Hg_{0.8}Bi_{0.2}$-1201 crystal from Ref. 7 is also given. On can note that T_c (onset) is lower (75 K) and that the transition width is larger, ΔT (10%–90%)=20 K. The T_c (onset)'s of 121 and 130 K for $Hg_{0.8}Bi_{0.2}$-1212 and $Hg_{0.8}Bi_{0.2}$-1223 crystals, respectively, were also confirmed from thermoremanent curves.

The crystal growth of 1212 and 1223 single crystals with similar [Hg/Bi] ratios offers a unique opportunity to compare their irreversibility lines (IL). In fact numerous studies have reported the irreversible properties of these phases for random crystallites of ceramic showing great discrepancies. For instance, at $t=T/T_c=0.6$, the irreversibility field (B_{irr}) of Hg-1212 was found to be 2 T (Ref. 9) or 0.4 T.[10] In order to limit the comparison with ceramics, we will only refer to studies of c-axis aligned materials measured in the $H\|c$ geometry.

Two sets of measurements were used in order to determine $B_{irr}(t=T/T_c)$ of the crystals. First $M(B)$ loops were recorded for different temperatures in the range 10–60 K for (Hg,Bi)-1212 and 15–90 K for (Hg,Bi)-1223, respectively. Typical plots are given in Fig. 7. For higher temperatures (corresponding to $B_{irr}<0.5$ T), zfc and fc $M(T)$ curves were registered in order to determine B_{irr}. An example corresponding to $B=0.03$ T for a $Hg_{0.8}Bi_{0.2}$-1212 crystal is given in Fig. 8 to attest the validity of the B_{irr}, T_{irr} measurements.

The corresponding irreversibility lines are reported in Fig. 9 where the IL of (Hg,Bi)-1201 is also shown. When looking at this latter graph, it is clear that the IL's of the 1212 phase lies below that of the 1223. Such a shift between the $n=2$ and $n=3$ members was also observed for thallium cuprate crystals between Tl monolayers, $TlBa_2Ca_{n-1}Cu_nO_{2n+3}$, and Tl bilayers, $Tl_2Ba_2Ca_{n-1}Cu_nO_{2n+4}$.[12] This clearly demon-

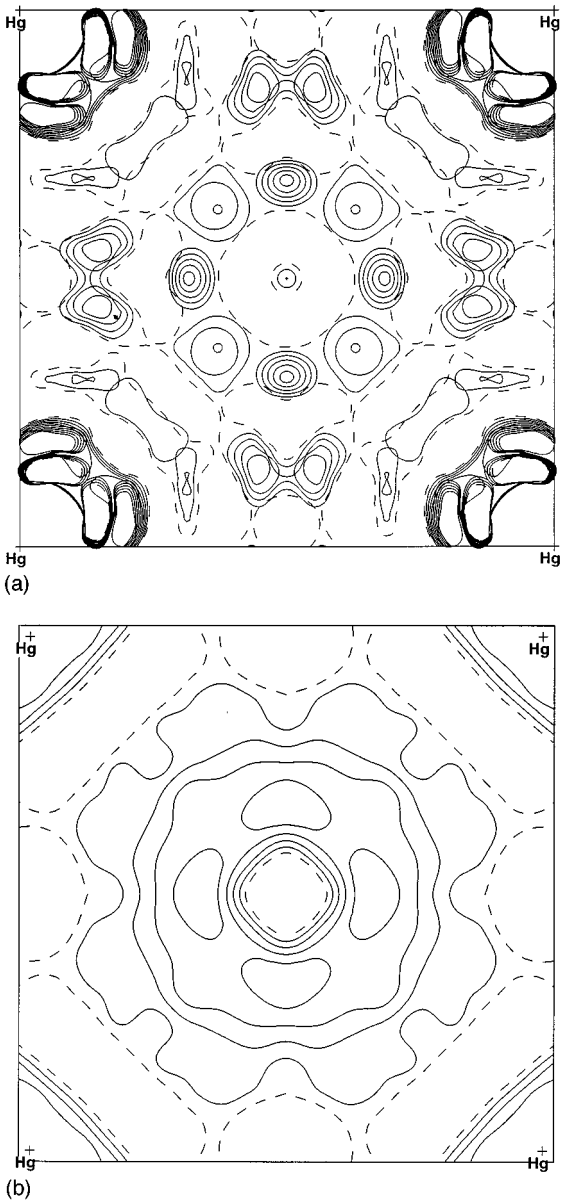

FIG. 3. (a) Electron density map for the $xy0$ section of $Hg_{0.8}Bi_{0.2}Ba_2CaCu_2O_{6+\delta}$ (1212). (b) Difference (001) Fourier map section at $z=0.0$, observed in $Hg_{0.8}Bi_{0.2}Ba_2CaCu_2O_{6+\delta}$ (1212), showing the splitting of the oxygen around the $(\frac{1}{2}\frac{1}{2}0)$ position

strates that $n=3$ compounds are better candidates for applications than $n=2$, since the former exhibit higher T_c's and IL's. However, the (Hg,Bi)-1201 IL lies in between those of the corresponding (Hg,Bi)-1212 and 1223 crystals. This peculiar behavior of the $n=1$ member was also observed in the case of the Tl bilayer cuprates; the properties of the $n=1$ member $Tl_2Ba_2CuO_6$ were optimized for crystals exhibiting an intermediate IL between the $n=2$ and $n=3$ members.[12] The same relation is observed for both (Hg,Bi) and Tl_2 series, i.e., $B_{\rm irr}(t)_{n=3}>B_{\rm irr}(t)_{n=1}>B_{\rm irr}(t)_{n=2}$.

Although the IL's of 1212 and 1223 are not located at the same position, their shapes are rather similar. For the highest fields ($B>0.3$ T), the IL's can be described by an exponential function if we consider the linearity observed in the semilogarithmic plots of Fig. 9. This is in agreement with a previous report of IL of Hg-1223 aligned powder, which also

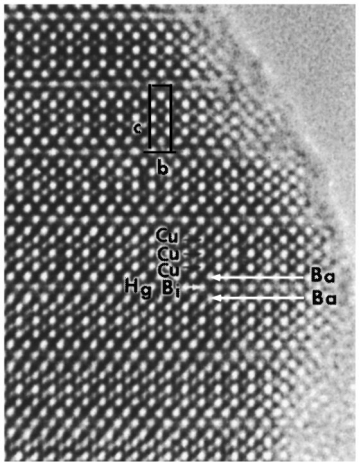

FIG. 4. [100] HREM image of the $Hg_{0.8}Bi_{0.2}Ba_2Ca_2Cu_3O_{8+\delta}$ (1223) single crystals fragments. The cations are imaged as bright dots (indicated on the right).

showed a crossover from this behavior to a power-law function.[13] Such a deviation is also observable from our data with corresponding fields of cross-over around 0.2–0.4 T in agreement with the value of Song *et al.*[13] Furthermore, a

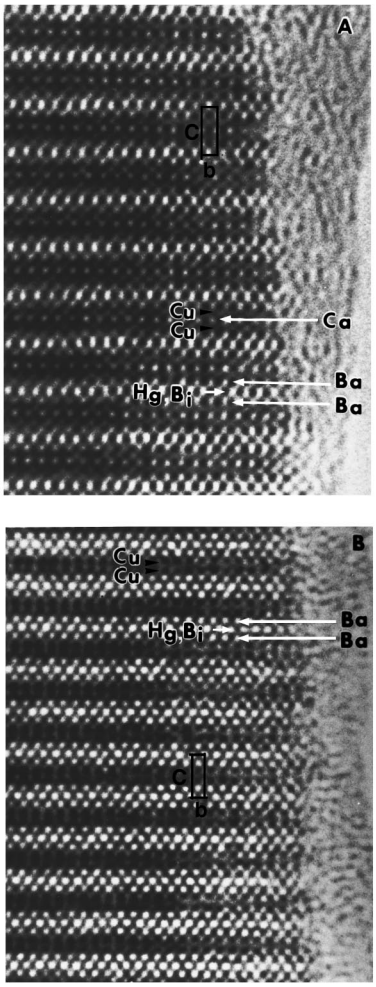

FIG. 5. [100] HREM image of the $Hg_{0.8}Bi_{0.2}Ba_2CaCu_2O_{6+\delta}$ (1212) single-crystal fragments: (a) The cations are imaged as dark dots (Focus value$=-250$ Å); (b) The cations are imaged as bright dots (Focus value$=-500$ Å).

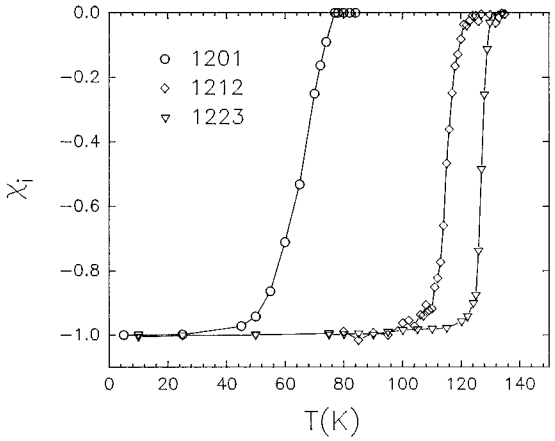

FIG. 6. T dependence of the internal susceptibility for $Hg_{0.8}Bi_{0.2}Ba_2CaCu_2O_{6+\delta}$ (1212), $Hg_{0.8}Bi_{0.2}Ba_2Ca_2Cu_3O_{8+\delta}$ (1223), and $Hg_{0.8}Bi_{0.2}Ba_2CuO_{4+\delta}$ (1201) crystals.

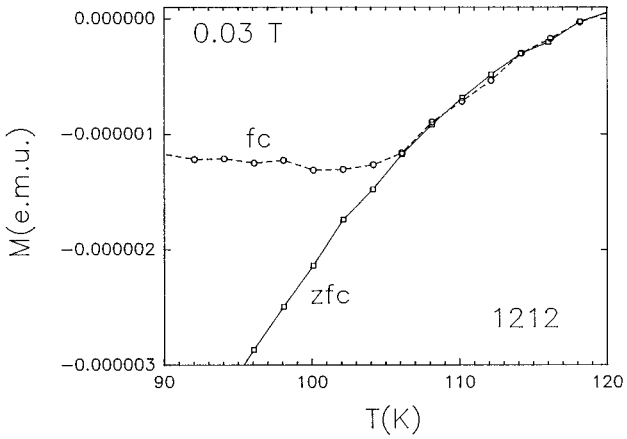

FIG. 8. zfc and fc curves registered with $B=0.03$ T for a $Hg_{0.8}Bi_{0.2}Ba_2CaCu_2O_{6+\delta}$ (1212) crystal. ($H\|c$).

good agreement with their irreversibility line location is found, $B_{irr}=1.7$ T at $T/T_c=0.5$ for $Hg_{0.8}Bi_{0.2}$-1223 crystal against $B_{irr}=2$ T at the same reduced temperature for their c-axis aligned powder. Finally, the most important result concerning the comparison between $Hg_{0.8}Bi_{0.2}$-1212 and $Hg_{0.8}Bi_{0.2}$-1223 IL's deals with the lower location of the former in the (H,T) plane. Another interesting result is related to the IL of $Hg_{0.8}Bi_{0.2}$-1223 single crystals which is quite similar to that of c-axis aligned powder Hg-1223, regarding their location or shape. This suggests that Bi doping on the mercury site does not modify significantly the IL location of Hg-1223.

However, the $M(B)$ loops registered for the Hg superconducting cuprates and for powders of ceramic (aligned or not) exhibit very different shapes. From the observation of Fig. 7, a fishtail shape is observed for the crystals in a limited T range but no such feature has been observed in ceramic studies. In contrast, at the same temperature, the shapes of $M(B)$ loops for Hg-1223 (c-axis aligned powder[15] or random crystallites[11,14]) exhibit decreasing field branches almost field independent with nearly zero magnitude.[14,15]

It was reported previously that the existence of fishtails is a general feature of crystals for the superconducting cuprate family (see Ref. 16, and references therein). The crystals of superconducting mercury cuprates corresponding to $n=1$, 2, and 3 confirm this rule. The temperature dependence of the B_{SP} magnetic field, where B_{SP} corresponds to the second peak of the decreasing branch of the hysteresis loop (see Fig. 7) are reported in Fig. 10 for $Hg_{0.8}Bi_{0.2}Ba_2CuO_{4+\delta}$, $Hg_{0.8}Bi_{0.2}Ba_2CaCu_2O_{6+\delta}$, and $Hg_{0.8}Bi_{0.2}Ba_2Ca_2Cu_3O_{8+\delta}$. As for $B_{irr}(t)$ lines, the same hierarchy is observed for the $n=2$ and $n=3$ members, i.e., $B_{SP}(t)_{1223}>B_{SP}(t)_{1212}$. One can also note that the $B_{SP}(t)_{1201}$ line position stands close to that of the 1212.

The fishtail shapes of the $M(B)$ loops have been previously interpreted[16] via models which imply a softening of the vortex lattice such as a 3D melting or more likely a 3D-2D decoupling.[17] By identifying the B_{SP} values with the crossover fields of these transitions which all obey the formula, $B=Af(t)\gamma^{-2}$,[16] the electronic anisotropy γ can be derived. As shown in Fig. 10, the fishtail lines of $Hg_{0.8}Bi_{0.2}$-1223 and Tl-1223 are close to each other. If one considers the $\lambda_{ab}(0)$

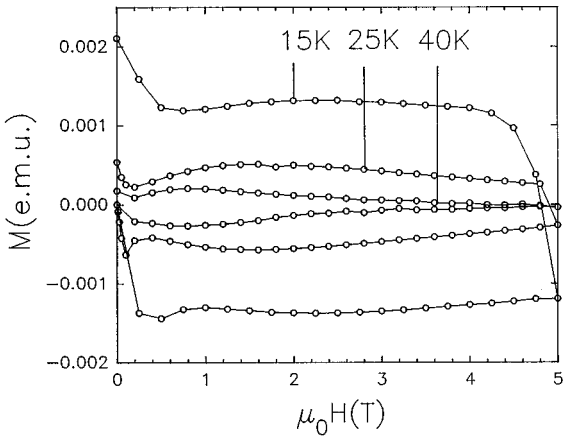

FIG. 7. Half hysteresis loops registered for a $Hg_{0.8}Bi_{0.2}Ba_2Ca_2Cu_3O_{8+\delta}$ (1223) crystal in the $H\|c$ geometry. T values are labeled on the graph.

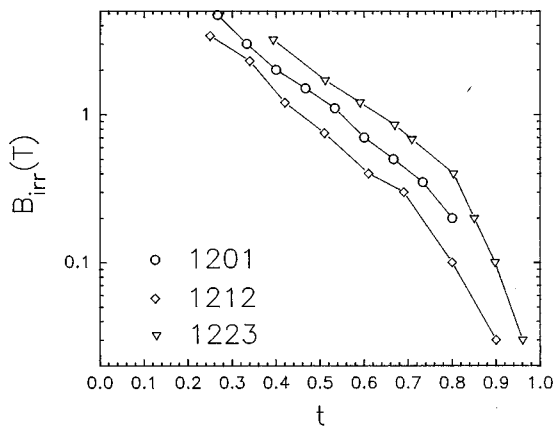

FIG. 9. Irreversibility lines for crystals of the $n=1$, 2, and 3 members of the $Hg_{0.8}Bi_{0.2}Ba_2Ca_{n-1}Cu_nO_{2n+2+\delta}$ series (t is the reduced temperature T/T_c).

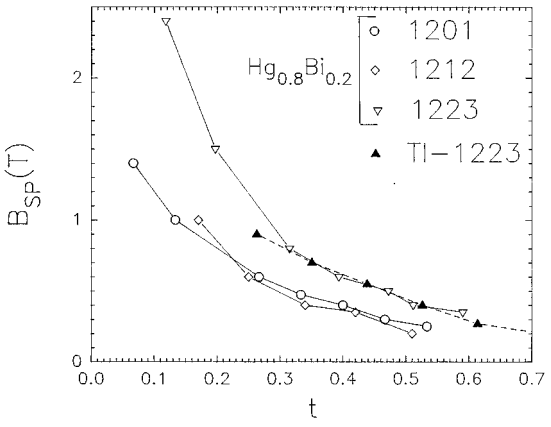

FIG. 10. $B_{SP}(t)$ lines corresponding to crystals of the $n=1$, 2, and 3 members of the $Hg_{0.8}Bi_{0.2}Ba_2Ca_{n-1}Cu_nO_{2n+2+\delta}$ series. The line of a Tl-1223 crystal (from Ref. 16) is also given.

values of these phases, $\lambda_{ab}(0)\sim1500$ Å for Hg-1223 single crystals,[5] i.e., close to the value of Tl-1223,[16] and their similar structural c parameters [$c\approx15.8$ Å for both (Hg,Bi)-1223 and Tl-1223] the similar location of their $B_{SP}(t)$ lines indicates that their anisotropies are very close. This suggests that the intrinsic nature of the fishtail is related to the structures whatever the thallium or mercury content. For Tl-1223 crystals, an anisotropy $\gamma=48$ was extracted from the $B_{SP}(t)$ line[16] and thus the anisotropy of $Hg_{0.8}Bi_{0.2}$-1223 may be close to this value. Such a value is also close to those established from torque magnetometry on single crystals for Hg-1223 ($\gamma=52$ Ref. 5) and for Hg-1234 ($\gamma=52$ Ref. 18). Nevertheless, it is difficult to discuss the effect of the CuO_2 plane number (n) on the γ values for our series. Indeed, the observed differences in the location of the $B_{SP}(t)$ lines for the three (Hg,Bi)-based compounds are quantitatively moderate. Thus, to compare their anisotropies one must use precise values of superconducting parameters such as λ_{ab} which could depend strongly on n as it has been previously reported on grain-aligned materials.[20] Measurements of the reversible magnetization of this (Hg,Bi) series of crystals are now in progress in order to establish their superconducting parameters.

CONCLUSION

The stabilization of Hg cuprates by Bi substitution has allowed the crystal growth of $Hg_{0.8}Bi_{0.2}Ba_2CaCu_2O_{6+\delta}$ (1212) and $Hg_{0.8}Bi_{0.2}Ba_2Cu_3O_{8+\delta}$ (1223) phases. These as-grown crystals exhibit T_c of 121 and 130 K for 1212 and 1223 respectively, indicating that after synthesis these crystals are nearly optimized since optimized $HgBa_2CaCu_2O_{6+\delta}$ and $HgBa_2Ca_2Cu_3O_{8+\delta}$ ceramics exhibit T_c's of 125 and 133 K respectively. This result differs from that obtained in the case of pure mercury $HgBa_2Ca_2Cu_3O_{8+\delta}$ crystals which exhibit as-grown T_c's of 105 K.[3] The magnetic properties study of both (Hg,Bi) cuprates has allowed a comparison of their irreversibility lines: in a reduced temperature scale, one observes that the $Hg_{0.8}Bi_{0.2}$-1212 IL position lies below that of $Hg_{0.8}Bi_{0.2}$-1223. Moreover the comparison with Hg-1223 c-axis aligned powder shows that the IL of $Hg_{0.8}Bi_{0.2}$-1223 is not strongly modified by the Bi introduction on the Hg sites. This result differs from studies of Pb-substituted Hg-1223 ceramics for which B_{irr} was found to be shifted higher by the substitution.[19] However, due to the random nature of the alignment of the latter ceramics, we cannot conclude definitively on the difference between the IL location observed for Bi and Pb substitution. Finally, the hysteresis loops of the crystals exhibit fishtail features in large T ranges which were not observed for ceramics samples. The most remarkable feature deals with the similar location of the fishtail lines for Tl-1223 and $Hg_{0.8}Bi_{0.2}$-1223 lines which rules out previous reports performed on ceramics claiming that the anisotropy of mercury cuprates was lower than that of thallium phases.

ACKNOWLEDGMENTS

The authors thank J. Chardon for the experimental contribution in the x-ray investigations. This work was supported by the Human Capital and Mobility program of the EEC.

*Author to whom correspondence should be addressed. Electronic address: physol@crismat.ismra.fr

[1] S. N. Putilin, E. V. Antipov, O. Chmaissen, and M. Marezio, Nature (London) **362**, 226 (1993).

[2] A. Schilling, M. Cantoni, J. D. Guo, and H. R. Ott, Nature (London) **363**, 56 (1993); O. Chmaissen, Q. Huang, S. N. Putilin, and A. Santoro, Physica C **212**, 259 (1993); S. M. Loureiro, E. V. Antipov, J-L. Tholence, J-J. Capponi, O. Chmaissen, Q. Huang, and M. Marezio, Physica C **217**, 253 (1993).

[3] D. Colson, A. Bertinotti, J. Hammann, J. F. Marucco, and A. Pinatel, Physica C **233**, 231 (1994).

[4] H. Schwer, J. Karpinski, K. Conder, L. Lesne, C. Rossel, A. Morawski, T. Lada, and A. Paszewin, Physica C **243**, 10 (1995).

[5] V. Vulcanescu, L. Fruchter, A. Bertinotti, D. Colson, G. Le Bras, and J. F. Marucco, Physica C **259**, 131 (1996).

[6] B. Raveau, C. Michel, M. Hervieu, and A. Maignan, J. Mat. Chem. **5**, 803 (1995); C. Michel, M. Hervieu, A. Maignan, D. Pelloquin, V. Badri, and B. Raveau, Physica C **241**, 1 (1995).

[7] D. Pelloquin, A. Maignan, A. Guesdon, V. Hardy, and B. Raveau, Physica C **265**, 5 (1996).

[8] L. W. Finger, R. M. Hazen, T. T. Downs, R. L. Meng, and C. W. Chu, Physica C **226**, 216 (1994).

[9] Z. J. Huang, Y. Y. Xue, R. L. Meng, and C. W. Chu, Phys. Rev. B **49**, 4218 (1994).

[10] U. Welp, G. W. Crabtree, J. L. Wagner, and D. G. Hinks, Physica C **218**, 373 (1993).

[11] A. Schilling, O. Jeandupeux, J. D. Guo, and H. R. Ott, Physica C **216**, 6 (1993).

[12] A. Wahl, V. Hardy, A. Maignan, C. Martin, and B. Raveau, Cryogenics **34**, 941 (1994); A. Wahl, Ph.D. thesis, University of Caen, 1995.

[13] Y. S. Song, M. Hirabayashi, H. Ihara, and M. Tokumoto, Phys. Rev. B **50**, 16 644 (1994).

[14] Y. R. Sun, J. R. Thompson, J. Schwartz, D. K. Christen, Y. C. Kim, and M. Paranthaman, Phys. Rev. B **51**, 581 (1995).

[15] Y. C. Kim, J. R. Thompson, D. K. Christen, Y. R. Sun, M. Paranthaman, and E. D. Specht, Phys. Rev. B **52**, 4438 (1995).

[16] V. Hardy, A. Wahl, A. Ruyter, A. Maignan, C. Martin, L. Coudrier, J. Provost, and Ch. Simon, Physica C **232**, 347 (1994).

[17] V. M. Vinokur, P. H. Kes, and A. E. Koshelev, Physica C **168**, 29 (1990); G. Deutscher and A. Kapitulnik, Physica A **168**, 338 (1990); L. I. Glazman and A. E. Koshelev, Phys. Rev. B **43**, 2835 (1991).

[18] D. Zech, J. Hofer, H. Keller, C. Rossel, P. Bauer, and J. Karpinski, Phys. Rev. B **53**, 6026 (1996).

[19] Z. Iqbal, T. Datta, D. Kirven, A. Lungn, J. C. Barry, F. J. Owens, A. G. Rinzler, D. Yang, and F. Reidinger, Phys. Rev. B **49**, 12 322 (1994); K. Isawa, A. Tokiwa-Yamamoto, M. Itoh, S. Adachi, and H. Yamauchi, Appl. Phys. Lett. **65**, 2105 (1994).

[20] R. Puzniak, K. Isawa, R. Usami, and H. Yamauchi, Physica C **233**, 21 (1994).